

Analytical approach to the single-domain-to-vortex transition in small magnetic disks

P.-O. Jubert and R. Allenspach

IBM Research, Zurich Research Laboratory, Säumerstrasse 4, CH-8803 Rüschlikon, Switzerland

(Received 29 April 2004; published 12 October 2004)

An analytical model to determine the stable configuration of thin ferromagnetic disks as a function of their thickness and diameter is presented. The vortex core energy is fully taken into account. The model includes materials with nonvanishing anisotropy. We find very good agreement with micromagnetic simulations provided that the energy of the finite difference calculation is corrected for the dipolar contribution arising from the discreteness at the edge.

DOI: 10.1103/PhysRevB.70.144402

PACS number(s): 75.75.+a, 75.60.Ch, 75.40.Mg

I. INTRODUCTION

Magnetic nanostructures have received considerable interest in recent years. Different magnetic configurations arise depending on size and shape of the element. In the smallest magnetic elements a single domain uniform configuration prevails. With increasing element size, deviations from uniformity arise and for small and intermediate anisotropy a transition from a single domain to a flux-closure configuration occurs. A thorough understanding of the single domain to flux-closure transitions is essential particularly for foreseen applications which aim to use single domain or vortex magnetic elements in high density magnetic data storage and spin-electronic devices.¹⁻³

In a given magnetic element, the configuration obtained at remanence is driven by the minimization of its magnetic energy. We neglect the magnetic history and focus on the lowest energy state without an applied magnetic field. This state can be reached for instance after appropriate demagnetization. Various experimental evidences of such transition exist in the literature, particularly in the case of magnetic disks. These are based on hysteresis loop studies⁴⁻⁶ or magnetic imaging^{7,8} on series of patterned elements. Theoretical comparison is usually given by a series of micromagnetic numerical simulations,⁹⁻¹¹ a technique that has proven to be an essential tool in this field. It has been used, for example, to show that the transition from a single domain to a vortex state can be rather complex in thin square elements with weak anisotropy, following a sequence of different configurations.¹² Analytical solutions of this micromagnetic problem are rare mainly due to the difficulty in treating the magnetostatic contribution of nonuniform configurations. They are, however, desirable as they allow trends to be predicted without the need to repeat the numerical simulation many times.

In this paper thin magnetic disks of thickness t and diameter S are considered that have variable in-plane magnetocrystalline anisotropy. The ratio t/S is kept smaller than 0.9 to avoid out-of-plane magnetization configurations,¹³ or more complicated three-dimensional vortex configurations.¹⁴ The possible magnetic states are then either the in-plane single domain (SD) or the vortex (V) configurations. We provide an analytical model to calculate which of these two magnetic states has the lower energy as a function of the disk

diameter and thickness. Compared to previous analytical approaches,¹⁵⁻¹⁷ the present model fully takes into account the vortex energy and is able to adequately describe vortex energy and width even for disk thicknesses smaller than the exchange length. The analytical approach is compared to micromagnetic simulations and we show that, depending on the anisotropy, this shifts the SD-V boundary towards a smaller or larger diameter. Finally we emphasize that inaccuracies appear in finite difference micromagnetic simulations in the evaluation of the energy because of the cell discretization which causes an intrinsic effective edge roughness. This effect has to be taken into account to correctly predict the SD-V boundary.

II. PRESENTATION OF THE ANALYTICAL MODEL

Let us first determine the analytical expressions of the magnetic energy for the SD state. When the magnetization is uniform and aligned along the in-plane easy axis of the thin disk its total magnetic energy equals the demagnetization energy

$$\varepsilon_{\text{tot}}^{\text{SD}} = \frac{1}{2} \mu_0 D_x M_s^2 \times (\pi S^2 t / 4). \quad (1)$$

M_s is the saturation magnetization and D_x is the demagnetization factor which is given by¹⁸

$$D_x = \frac{1}{2} \left\{ 1 - \frac{S}{t} \left[\frac{4}{3\pi} - \int_0^\infty dx \left(\frac{J_1(x)}{x} \right)^2 \exp\left(-\frac{2t}{S}x\right) \right] \right\}, \quad (2)$$

where $J_1(x)$ denotes the first order Bessel function. For $t/S \ll 1$, Eq. (2) can be approximated by¹⁸

$$D_x \approx \frac{t}{\pi S} \left[\ln\left(4\frac{S}{t}\right) - 0.5 \right]. \quad (3)$$

Let us now express the total magnetic energy when the magnetic configuration in the disk is a vortex. When t is small compared to the exchange length, the vortex magnetization distribution is essentially constant throughout the thickness.¹⁹ Typically, this is expected for $t \leq 10 \lambda_{\text{exch}}$ with $\lambda_{\text{exch}} = \sqrt{2A_{\text{exch}} / \mu_0 M_s^2}$ and A_{exch} the exchange constant. Then, the magnetization normalized by M_s can be expressed in cylindrical coordinates

$$m_\rho = 0, m_\varphi = [1 - m_z(\rho)^2]^{1/2}, m_z = m_z(\rho). \quad (4)$$

The exchange energy density, the uniaxial anisotropy and the cubic fourfold anisotropy energy densities are then given, respectively, by

$$e_{\text{exch}} = A_{\text{exch}} \left[(\partial m_z / \partial \rho)^2 \frac{1}{1 - m_z^2} + (1 - m_z^2) / \rho^2 \right], \quad (5)$$

$$e_{K_u} = K_u \{ \sin^2(\varphi) [1 - m_z(\rho)^2] \}, \quad (6)$$

$$e_{K_c} = K_c \{ \cos^2(\varphi + \Delta\varphi) \sin^2(\varphi + \Delta\varphi) [1 - m_z(\rho)^2]^2 + m_z(\rho)^2 [1 - m_z(\rho)^2]^2 \}, \quad (7)$$

where K_u and K_c are the uniaxial and cubic anisotropy constant, respectively, and $\Delta\varphi$ is the angle between the easy axes given by the uniaxial and the cubic anisotropy. Integration over the volume of the disk leads to the exchange ($\varepsilon_{\text{exch}}$) and the anisotropy contributions ($\varepsilon_{K_u}, \varepsilon_{K_c}$) of the total magnetic energy $\varepsilon_{\text{tot}}^V = \varepsilon_{\text{exch}} + \varepsilon_{K_u} + \varepsilon_{K_c} + \varepsilon_{\text{dem}}$. The evaluation of the magnetostatic energy ε_{dem} is complex and numerical evaluation is usually required. For an ideal vortex configuration in a disk it is, however, possible to derive an analytical expression for the magnetostatic energy²⁰

$$\varepsilon_{\text{dem}} = \pi \mu_0 M_s^2 \int_0^\infty (1 - e^{-\alpha t}) \left[\int_0^\infty \rho m_z(\rho) J_0(\alpha \rho) d\rho \right]^2 d\alpha. \quad (8)$$

Both energy and magnetization profile of the vortex configuration are found by minimizing $\varepsilon_{\text{tot}}^V = \varepsilon_{\text{exch}} + \varepsilon_{K_u} + \varepsilon_{K_c} + \varepsilon_{\text{dem}}$ with the adequate $m_z(\rho)$ function. For this variational problem, Feldtkeller and Thomas chose the ansatz $m_z = \exp(-2\rho^2\beta^2)$, with the minimization parameter $1/\beta$ corresponding to the width of the vortex.²⁰ We will compare this approach to other recent choices^{15,21} for $m_z(\rho)$ below.

The different energy terms are then given by

$$\varepsilon_{\text{exch}} = \pi A_{\text{exch}} t \left(\frac{\pi^2}{6} + \ln(\gamma \beta^2 S^2) \right), \quad (9)$$

$$\varepsilon_{K_u} = \frac{K_u}{2} \pi t \left(\frac{S}{2} \right)^2 \left[1 - \frac{1}{\beta^2 S^2} (1 - e^{-\beta^2 S^2}) \right], \quad (10)$$

$$\varepsilon_{K_c} = \frac{K_c}{8} \pi t \left(\frac{S}{2} \right)^2 \left[1 + \frac{6}{\beta^2 S^2} (1 - e^{-\beta^2 S^2}) - \frac{7}{2\beta^2 S^2} (1 - e^{-2\beta^2 S^2}) \right] \quad (11)$$

and, assuming a small vortex width compared to the disk diameter ($\beta S \gg 1$),

$$\varepsilon_{\text{dem}} = \frac{\pi^{3/2} \mu_0 M_s^2}{16\beta^3} \{ 1 - \exp(\beta^2 t^2) [1 - \text{Erf}(\beta t)] \} \quad (12)$$

with $\text{Erf}(x)$ the error function, and $\ln(\gamma) = 0.5772\dots$, the Euler constant. The vortex configuration profile and its related energy can finally be determined by minimizing $\varepsilon_{\text{tot}}^V$ as a function of β . For thin disks we can use a constant β as a

first approximation, $\beta = \sqrt{1 + (K_u + 5K_c/8) / (\mu_0 M_s^2)} / (2\lambda_{\text{exch}})$, which is exact in the limit of an infinitely thin disk.²⁰ The validity of this approximation for determining the SD- V boundary is demonstrated below. Within these approximations the total magnetic energy of a disk, being either in a perfect uniform or vortex configuration, is expressed analytically as a function of the material parameters and of the dimensions of the disk.

For any given diameter and thickness the energetically preferred configuration can be calculated, leading to the phase diagram of the equilibrium domain configurations. The curve separating the single domain from the vortex state is finally determined from numerically solving $\varepsilon_{\text{tot}}^{\text{SD}}(S, t) = \varepsilon_{\text{tot}}^V(S, t)$.

III. DETAILS OF THE MICROMAGNETIC SIMULATIONS

The analytic model is compared to micromagnetic simulations performed using the OOMMF package.²² The material parameters $M_s = 1424$ kA/m and $A_{\text{exch}} = 30 \times 10^{-12}$ J/m used here correspond to those of Co small elements epitaxially grown on vicinal Cu(001) crystals that we investigate experimentally. However, both analytical and simulation results are scaled by $\lambda_{\text{exch}} = 4.85$ nm so that the results are independent of the choice of material parameters. The disks are discretized into cubic cells 2.5 nm in size, corresponding to half the exchange length. For simplicity we consider only uniaxial anisotropy contributions although uniaxial and cubic anisotropy could be taken into account in the model if required. The results are very similar in terms of configuration energy with cubic anisotropy because $\beta S \gg 1$: An almost constant energy adds to the vortex energy which takes the role of an additional uniaxial anisotropy $K_u^{\text{eff}} = K_c/4$ [see Eqs. (10) and (11)].

IV. RESULTS AND DISCUSSION

Figure 1 compares the SD- V boundary determined from the analytical model and from a set of micromagnetic simulations. Very good agreement is found with different anisotropy values which demonstrates the accuracy of our analytical approach.

The SD state is lower in energy as long as the magnetostatic energy caused by the lack of flux closure is less than the vortex energy. For thinner elements the SD to V transition arises at larger element sizes since the magnetostatic energy is less dominant. A peculiar reentrant behavior is found for large anisotropy constants and thicknesses in the order of the exchange length: The lower energy configuration changes from SD to V and eventually back to SD at large disk diameters. The first transition results from the competition between the exchange energy in the V state and the dipolar energy of the SD state. The second transition occurs at large disk dimensions when the V state energy, then dominated by anisotropy $E_{\text{tot}}^V \simeq \varepsilon_{\text{anis}} \propto S^2$, becomes larger than the SD state energy $E_{\text{tot}}^{\text{SD}}$ proportional to $S \ln(S)$ [see Eqs. (1)–(3) and (10)].

Small discrepancies in the position of the boundary are observed between the analytical approach and the simula-

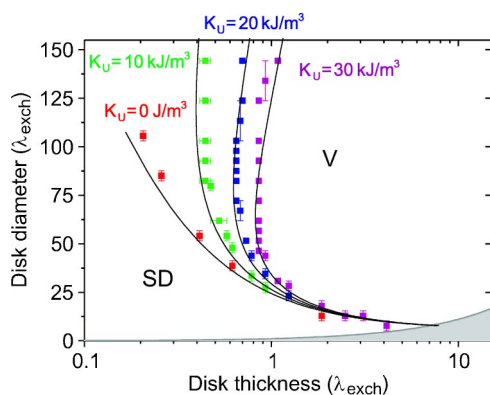


FIG. 1. (Color online) SD-V boundary for disks of diameter S and thickness t with varying uniaxial anisotropy ($K_u=0$ kJ/m³, $K_u=10$ kJ/m³, $K_u=20$ kJ/m³, and $K_u=30$ kJ/m³). Lines correspond to the analytical model, dots to micromagnetic simulations. The error bars estimate the inaccuracy of the simulation results introduced by the fact that the simulations were done on a finite grid in the (S, t) parameter space. The gray area shows the region in which the out-of-plane SD state prevails over the in-plane SD state (Ref. 13).

tions, particularly in the large disk diameters. These occur as the model does not take possible local deviations in the magnetization into account. The single domain configuration is assumed to be a homogenous, uniform state. However, micromagnetic simulations reveal that local deviations can be introduced for large diameters, see Fig. 2. While such deviations come with a cost in exchange and anisotropy energy, demagnetization energy is gained. Similarly the vortex magnetization is assumed to have a perfect cylindrical symmetry. This is entirely correct in the case of weak anisotropy systems but with larger anisotropy and with larger diameters, deviations occur (see Fig. 2). Such local deviations lower the vortex energy as soon as the gain in anisotropy and exchange energy exceeds the cost of demagnetization energy. For both the SD state and the V state, the importance of these deviations depends on the strength of the anisotropy but in opposite directions. For weak anisotropy, the vortex configuration deviates weakly from a cylindrical distribution. The analytical approach then leads to a lower boundary of the SD-V transition as clearly observed in Fig. 1. In contrast, for large anisotropy the uniform SD configuration is stabilized by the anisotropy while strong deviations to the cylindrical distribution appear in the vortex state: The analytical model then tends to be an upper bound of the SD-V transition.

V. THE INACCURACY OF MICROMAGNETIC SIMULATIONS CAUSED BY DISCRETIZATION

The relevance of the analytical model is tested by a comparison to micromagnetic simulations using a finite difference method. The simulations precisely determine the equilibrium configuration, which is not necessarily the perfect SD or perfect V state. However, the discreteness of the method and the use of a cubic mesh is the origin of systematic errors for nonrectangular systems. This is particularly true for disks since the circular boundary is approximated by

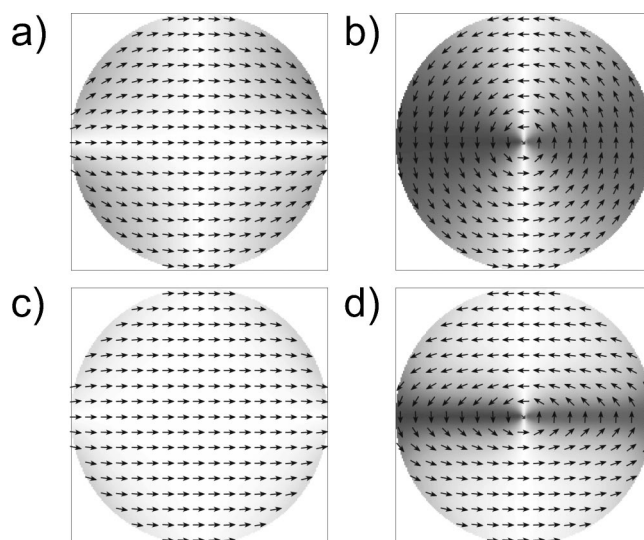


FIG. 2. Calculated single domain (a), (c) and vortex (b), (d) configurations for a disk 500 nm in diameter and 1 nm in thickness. (a), (b) $K_u=0$ and (c), (d) $K_u=30$ kJ/m³. The easy magnetization axis lies along the horizontal. Gray levels correspond to the absolute magnetization component along the vertical.

a staircase of straight-line segments. This artificial edge roughness introduces surface charges which increase the demagnetization energy. Figure 3 shows this contribution from the outer boundary of the disk for the vortex configuration with $K_u=0$.

This additional dipolar energy is determined by extracting the demagnetization energy of the disk edges in the case of a perfect cylindrical vortex. It is proportional to the disk perimeter length and rapidly increases with cell size as illustrated in Fig. 3(c). For the small cell size of 2.5 nm and $S=300$ nm, $t=2$ nm, it already amounts to 15% of the total energy and exceeds the intrinsic demagnetization energy by a factor of 1.6. This systematic overestimation of the demagnetization energy in the V state is particularly problematic because it leads to a shift in the SD-V boundary, as shown in Fig. 4 for $K_u=0$. Thus it is crucial to determine numerical edge-roughness effects when using finite difference micromagnetic simulations for calculating the energy of nonrectangular systems.

VI. COMPARISON WITH OTHER MODELS AND EXPERIMENTAL VALUES

Figure 5 compares the calculated SD-V boundary for $K_u=0$ with the results from other models reported in the literature.^{15–17} In Ref. 15 the vortex energy is calculated without taking the vortex core into account. This leads to a systematic overestimation of the energy of the vortex state which shifts the SD-V boundary towards larger disk diameters, see Fig. 5. Although the vortex core is small compared with the disk diameter, it significantly reduces the vortex-state energy: It leads to a large reduction in the exchange energy of the disk center at the expense of a small dipolar energy increase. Note that this model was also compared to finite difference micromagnetic simulations,¹⁵ however, as

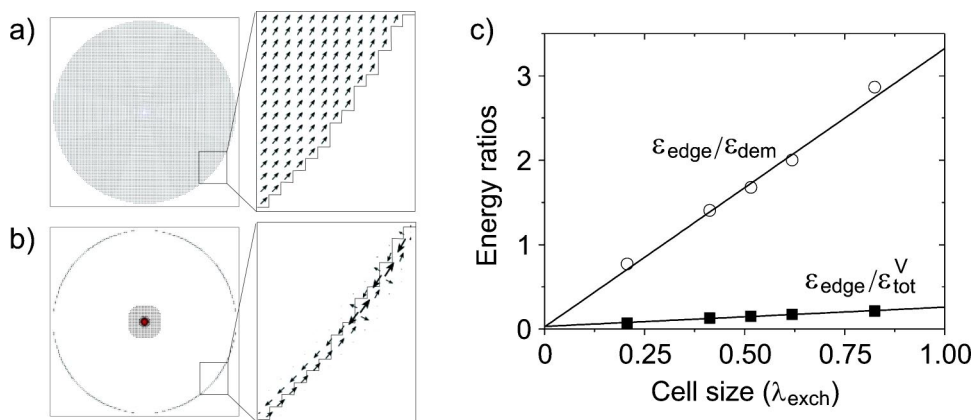


FIG. 3. (a) Magnetization distribution calculated for the V state configuration in a disk with $K_u=0$, $S=300$ nm, and $t=2$ nm. The zoom shows the numerical edge roughness of the disk. (b) Dipolar field distribution calculated for the same disk. (c) Ratio of edge-roughness dipolar energy ϵ_{edge} to demagnetization ϵ_{dem} and total energy ϵ_{tot}^V as a function of cell size for the same disk dimensions.

the edge roughness was not taken into account the simulations overestimated the vortex state energy and hence led to a fortuitous agreement between analytical model and simulations.

The calculation of the V -state energy requires a correct description of the vortex core. Decades after the work by Feldtkeller and Thomas²⁰ an alternative description of the vortex core based on a variational principle was proposed by Usov and Peschany.²¹ For $m_z(\rho)$ they propose a noncontinuous function $m_z(\rho)=(a^2-\rho^2)/(a^2+\rho^2)$ for $\rho < a$ and $m_z(\rho)=0$ for $\rho \geq a$. The variational parameter a takes the role of the core width and has to be determined from a minimization of the demagnetizing and the exchange energy. The authors of Ref. 21 restrict the calculation to the case $a < t$, such that the part of the magnetostatic energy term which corresponds to the interaction of the poles of the opposite surfaces can be neglected. The analytical formula of Ref. 21 is a good approximation of the vortex core width for $t > 2\lambda_{\text{exch}}$ but underestimates it at small thickness. This is confirmed in Fig. 6

where the calculated vortex core width is compared to a set of micromagnetic simulations. As a result, the SD- V boundary calculated by this approach^{16,17} is shifted towards larger disk diameters of small thickness, see Fig. 5.

In contrast, the Feldtkeller and Thomas ansatz gives a very good approximation of the vortex core width at all thicknesses. Therefore it allows a better estimation than the other models for the SD- V boundary of magnetic disks, particularly at small thicknesses. Since we are interested in ultrathin disks, we have omitted the variational determination of the core width at each thickness and approximated the core width by the zero-thickness limit. Figure 6 shows that such an approximation correctly describes the core width for $t < 2\lambda_{\text{exch}}$. Although the core width at larger thicknesses is slightly underestimated with the zero-thickness approximation, the SD- V boundary is not significantly affected. It gives, for instance, an energy difference of 2.5% for the vortex state for $K_u=0$ with $S=200$ nm and $t=20$ nm $\approx 4\lambda_{\text{exch}}$. This is similar to the -2% energy difference found between the analytical model and both our finite difference calcula-

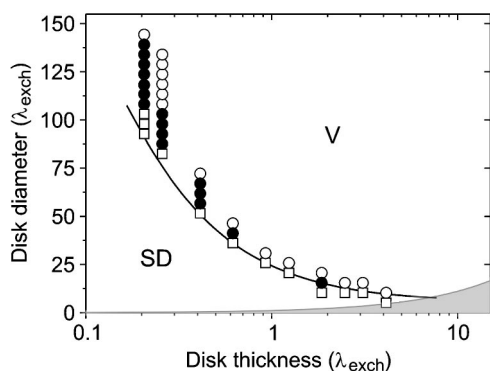


FIG. 4. Lower energy configurations as a function of disk diameter and thickness determined from micromagnetic simulations with $K_u=0$. Squares: the SD state is more stable; Open circles: the V state is more stable. Filled circles: the V state is the lower energy state, only when the V -state energy is corrected from the artificial edge-roughness dipolar contribution. The SD- V boundary determined from the analytical model is given by the line. The gray area shows the disk dimensions where the out-of-plane SD state prevails over the in-plane SD state (Ref. 13).

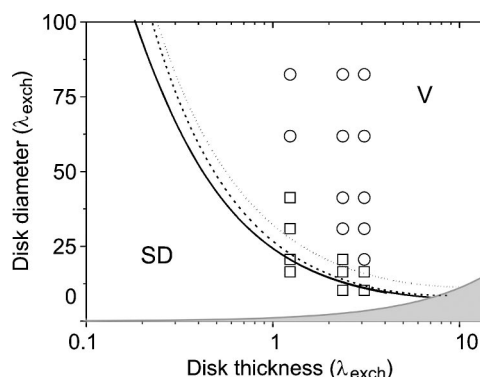


FIG. 5. Comparison of the SD- V boundary for disks without anisotropy determined with our analytical model (solid line), the model of Ref. 15 (dotted line), and the model using the vortex description of Ref. 21 (dashed line). Experimental stable configurations observed for $\text{Fe}_{20}\text{Ni}_{80}$ disks (Ref. 12) are also displayed with squares corresponding to the single-domain state and circles to the vortex states. The gray area shows the region in which the out-of-plane SD state prevails over the in-plane SD state (Ref. 13).

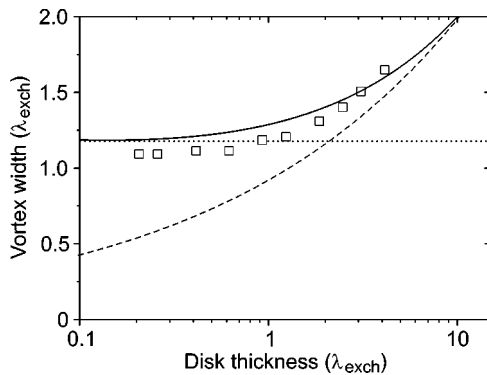


FIG. 6. Vortex core width at $m_z=0.5$ as a function of disk thickness t determined from the variational approach by Feldtkeller and Thomas (Ref. 20) (solid line) and from the analytical formula by Usov and Peschany (Ref. 21) (dashed line). The limiting value of Feldtkeller and Thomas at zero thickness is the approximation used in this paper (dotted line). The results of the micromagnetic simulations are given by squares, with a disk diameter of 400 nm.

tion (corrected from numerical edge roughness) and the finite element calculation results of Ref. 17. The corresponding shift of the SD-V boundary at large thickness is too small to be discerned in Fig. 5.

Figure 5 also compares the SD-V boundary with experimental results on patterned $\text{Fe}_{20}\text{Ni}_{80}$ disks with negligible anisotropy.⁵ The evolution of the lower energy configuration with disk thickness and diameter is in good agreement with the model. However, as already stated in the original work,⁵

the micromagnetic simulations are found to have a lower limit for the SD-V boundary when compared with the experimental results. A possible additional weak anisotropy does not explain this discrepancy. Following the analysis of the micromagnetic simulations presented above, a more likely explanation could be experimental edge roughness. Alternatively, the configuration observed at zero field is not necessarily the true equilibrium configuration, as it may depend on the way the remanence state has been reached.

VII. CONCLUSION

In this paper, an analytical model is described that allows the lower energy configuration for thin magnetic disks to be calculated at zero field. For a given set of material parameters, the transition from SD to V configurations is determined analytically as a function of the disk diameter and thickness. The result of this analytical approach is compared with micromagnetic simulations. The model is shown to provide a very good estimate of the SD-V transition without the need of long and numerous micromagnetic calculations. Small discrepancies are found at large disk diameters as deviations from a purely uniform or cylindrical configuration may arise. Depending on the material anisotropy, the SD-V boundary is slightly moved towards the SD or the V phase. Inaccuracies in the vortex energy calculation of a disk were identified in micromagnetic simulations. They are due to intrinsic numerical edge roughness that needs to be carefully taken into account in micromagnetic problems.

¹G. A. Prinz, *Science* **282**, 1660 (1998).

²R. L. White, *J. Magn. Magn. Mater.* **242-245**, 21 (2002).

³W. J. Gallagher, S. S. P. Parkin, Y. Lu, X. P. Bian, A. Marley, K. P. Roche, R. A. Altman, S. A. Rishton, C. Jahnes, T. M. Shaw, and G. Xiao, *J. Appl. Phys.* **81**, 3741 (1997).

⁴C. Miramond, C. Fermon, F. Rousseaux, D. Decanini, and F. Carcenac, *J. Magn. Magn. Mater.* **165**, 500 (1997).

⁵R. P. Cowburn, D. K. Koltsov, A. O. Adeyeye, M. E. Welland, and D. M. Tricker, *Phys. Rev. Lett.* **83**, 1042 (1999).

⁶M. Schneider and H. Hoffmann, *J. Appl. Phys.* **86**, 4539 (1999).

⁷A. Fernandez, M. R. Gibbons, M. A. Wall, and C. J. Cerjan, *J. Magn. Magn. Mater.* **190**, 71 (1998).

⁸M. Schneider, H. Hoffmann, and J. Zweck, *Appl. Phys. Lett.* **77**, 2909 (2000).

⁹W. Rave, K. Fabian, and A. Hubert, *J. Magn. Magn. Mater.* **190**, 332 (1998).

¹⁰N. Dao, S. L. Whittenburg, and R. P. Cowburn, *J. Appl. Phys.* **90**, 5235 (2001).

¹¹C. A. Ross M. Hwang, M. Shima, J. Y. Cheng, M. Farhoud, T. A. Savas, H. I. Smith, W. Schwarzacher, F. M. Ross, M. Redjail,

and F. B. Humphrey, *Phys. Rev. B* **65**, 144417 (2002).

¹²R. P. Cowburn and M. E. Welland, *Appl. Phys. Lett.* **72**, 2041 (1998).

¹³A. Aharoni, *J. Appl. Phys.* **68**, 2892 (1990).

¹⁴J. K. Ha, R. Hertel, and J. Kirschner, *Phys. Rev. B* **67**, 064418 (2003).

¹⁵H. Hoffmann and F. Steinbauer, *J. Appl. Phys.* **92**, 5463 (2002).

¹⁶K. L. Metlov and K. Y. Guslienko, *J. Magn. Magn. Mater.* **242-245**, 1015 (2002).

¹⁷W. Scholz, K. Y. Guslienko, V. Novosad, D. Suess, T. Schrefl, R. W. Chantrell, and J. Fidler, *J. Magn. Magn. Mater.* **266**, 155 (2003).

¹⁸R. I. Joseph, *J. Appl. Phys.* **37**, 4639 (1966).

¹⁹A. Hubert and R. Schäfer, *Magnetic Domains. The Analysis of Magnetic Microstructures* (Springer-Verlag, Berlin, 1998).

²⁰E. Feldtkeller and H. Thomas, *Phys. Kondens. Mater.* **4**, 8 (1965).

²¹N. A. Usov and S. E. Peschany, *J. Magn. Magn. Mater.* **118**, L290 (1993).

²²M. J. Donahue and D. G. Porter, <http://math.nist.gov/oommf/>